



ELSEVIER

Surface Science 382 (1997) L666–L671

surface science

Surface Science Letters

# The structure and phase stability of CO adsorbates on Rh(110)

Dario Alfè<sup>a</sup>, Stefano Baroni<sup>a,b,\*</sup><sup>a</sup> *INFN (Istituto Nazionale di Fisica della Materia) and SISSA (Scuola Internazionale di Studi Superiori ed Avanzati), via Beirut 2–4, 34014 Trieste, Italy*<sup>b</sup> *CECAM, ENSL, Aile LRS, 46 Allée d'Italie, 69364 Lyon, Cedex 07, France*

Received 11 October 1996; accepted for publication 18 February 1997

## Abstract

The structure of CO adsorbates on the Rh(110) surface is studied at full coverage using first-principles techniques. The relative energies of different adsorbate geometries are determined by means of accurate structure optimizations. In agreement with experiments, we find that a  $p2mg(2 \times 1)$ -2CO structure is the most stable. The CO molecules sit on the short-bridge site (carbon below) with the molecular axis slightly tilted off the surface normal, along the (001) direction. Configurations corresponding to different distributions of tilt angles are mapped onto an anisotropic two-dimensional Ising model whose parameters are extracted from our ab initio calculations. We find that an order–disorder phase-transition occurs at a temperature  $T_c \approx 300$  K. © 1997 Elsevier Science B.V.

**Keywords:** Carbon monoxide; Chemisorption; Density functional calculations; Ising models; Rhodium; Surface thermodynamics

Rhodium surfaces are attracting a wide scientific and technological interest due to their catalytic properties, particularly because they act so as to reduce the energy activation barrier for the reaction  $2CO + 2NO \rightarrow 2CO_2 + N_2$ , and thus to eliminate the two poisonous CO and NO gases from the pollution emission of combustion engines.

The stable structure of the Rh(110) clean surface is unreconstructed. However, if prepared in a convenient way with oxygen adsorption it may also present – upon thermal desorption – metastable  $(1 \times n)$  ( $n=2, 3, 4, 5$ ), missing- or added-row structures which revert to the unreconstructed one at temperatures  $>480$  K [1–3].

The adsorption of CO molecules on Rh(110) has been studied experimentally by means of a

variety of techniques [4–12]. The adsorption of 1 monolayer (ML) of carbon monoxide on the unreconstructed surface results in a  $(2 \times 1)p2mg$  structure, with the C atom bound in the short-bridge sites along the  $(1\bar{1}0)$  direction, and the molecular axis alternatively tilted with respect to the surface normal, towards the (001) direction [9]. In Ref. [6], the  $(2 \times 1)p2mg$  low energy diffraction (LEED) pattern was reported to disappear at temperatures higher than  $\approx 270$ – $280$  K, well below the desorption of CO from the surface. This fact was tentatively explained in terms of an order–disorder phase-transition.

In this paper the structure and phase stability of 1 ML of CO molecules adsorbed on the Rh(110)- $(1 \times 1)$  surface are studied from first principles and by mapping the low-lying energy configurations corresponding to the different distri-

\* Corresponding author.

butions of tilt angles onto an anisotropic two-dimensional Ising model. The latter is then simulated using a standard Metropolis Monte Carlo algorithm. The order–disorder transition temperature estimated from our simulations is  $\approx 300$  K, in fair agreement with experimental findings [6].

Our calculations are based on density functional theory within the local-density approximation (LDA) [13,14], using Ceperley–Alder correlation energies [15]. The one-particle Kohn–Sham equations are solved self-consistently using plane-wave (PW) basis sets in a pseudopotential scheme. Because of the well-known *hardness* of the norm-conserving (NC) pseudopotentials for the O and – to a lesser extent – Rh atoms, we make use of *ultra-soft* (US) pseudopotentials [16] which allow an accurate description of the O and Rh valence pseudo-wavefunctions with a modest basis set including PWs up to a kinetic-energy cutoff of 30 Ry. In the case of Rh, we found it convenient to treat the s and p channels using a NC potential, while the US scheme is applied only to the *hard* d orbital [17,18]. With such a small basis set, the accuracy is slightly improved if C is also treated within the US scheme, which we decided to do. Brillouin-zone (BZ) integrations are performed using the Gaussian-smearing [19] special-point [20] technique. In agreement with Ref. [18], we find that the structural properties of bulk Rh are well converged using a first-order Gaussian smearing function [19] of width  $\sigma=0.03$  Ry and ten special  $\mathbf{k}$ -points in the irreducible wedge of the BZ (IBZ). The isolated surface is modeled by a periodically repeated super-cell. We have used the same super-cell for both the clean and the CO-covered surfaces. For the clean surface we have used seven atomic layers plus a vacuum region corresponding to ca nine layers. For the CO-covered surface the seven Rh layers are completed by one layer of CO molecules on each side of the slab: in this case the vacuum region is correspondingly reduced to  $\approx 5.5$  atomic layers. We have used the same Gaussian-smearing function as in the bulk calculations with eight special  $\mathbf{k}$ -points in the surface IBZ. Convergence tests performed with a value of  $\sigma$  twice as small and a correspondingly finer mesh of special points resulted in no significant changes in total energies and equilibrium geometries. The

latter are found by allowing all the atoms in the slab to relax until the force acting on each of them is smaller than  $0.5 \times 10^{-3}$  Ry  $a_0^{-1}$ .

The clean Rh(110) surface is unreconstructed. An analysis of LEED data suggests that the top interlayer spacing is reduced by  $6.9 \pm 1.0\%$  relative to the bulk interlayer spacing, while the second interlayer spacing would expand by  $1.9 \pm 1.0\%$  [21]. Our ab initio data indicate a relaxation of  $-9\%$  and of  $3.5\%$  in the first and second interlayer spacings, respectively, while the interlayer spacings beyond the second are practically unchanged.

For the CO-covered surface, LEED data indicate that the molecules are bound in the short-bridge site between two first layer Rh atoms in the (001) direction with the molecular axis tilted by  $24 \pm 4^\circ$  from the surface normal, forming a  $(2 \times 1)p2mg$  structure. In principle there are many different ways to arrange the CO molecules so as to obtain the same LEED pattern. We concentrate our attention on three possible adsorption sites:

- (1) the *short-bridge* one described above;
- (2) the *on-top* one, in which the CO molecule is located on top of the first-layer atoms; and
- (3) the *hollow* site, formed by two first-layer atoms in the (001) direction and one second-layer atom.

In agreement with the outcome of the LEED analysis, we find that the short-bridge site is the most favorable. The relative energies of the other two sites with respect to the short-bridge – assuming a  $(1 \times 1)$  structure in all cases – are: 0.19 eV (hollow) and 0.34 eV (on-top). We find that the angle between the surface normal and the CO molecular axis is  $\alpha = 17 \pm 2^\circ$ , and that the angle between the Rh–C bond and the surface normal is  $\delta = 13 \pm 2$  degrees; the Rh–C bond length is 2.02 Å, and the C–O distance is 1.17 Å. The Rh substrate presents an outward relaxation of the first layer of 2.8% with respect to the bulk interlayer spacing. These results are summarized in Table 1 together with similar ones obtained for six other different surface geometries (see Fig. 1). From Table 1 we see that the  $(1 \times 1)$  and  $(1 \times 2)$  geometries are degenerate within our error bar which we estimate to be  $\pm 1$  meV per molecule, and that the uncertainty on the corresponding tilt angle is very large. This behavior can be under-

Table 1  
Structural data for seven different surface structures (see Fig. 1)<sup>a</sup>

	$\alpha$ (°)	$\delta$ (°)	$d(\text{C-O})$ (Å)	$d(\text{Rh-C})$ (Å)	$\Delta E$ (meV per molecule)
Expt	$24 \pm 4^b$	$13 \pm 4^b$	$1.13 \pm 0.09^b$	$1.97 \pm 0.09^b$	
$2 \times 1$	$17 \pm 2$	$13 \pm 2$	1.17	2.02	0.0
$1 \times 1$	$\leq 10$	$\leq 10$	1.17	2.02	33.5
$1 \times 2$	$\leq 5$	$\leq 5$	1.17	2.02	33.5
$2 \times 2$	$13 \pm 2$	$11 \pm 2$	1.17	2.02	13.5
$2 \times 2'$	$13 \pm 2$	$11 \pm 2$	1.17	2.02	21.5
$4 \times 1$	$16 \pm 2$	$13 \pm 2$	1.17	2.02	17.0
$4 \times 1'$	$16 \pm 2$	$12 \pm 2$	1.17	2.02	17.0

<sup>a</sup> $\alpha$  and  $\delta$  are the angles between the surface normal and the C–O and the Rh–C axis, respectively.  $\Delta E$  is the energy difference per molecule between the ( $n \times m$ ) and the ( $2 \times 1$ ) structures. The theoretical error is estimated to be  $\approx 2$  meV. The experimental values refer to the ( $2 \times 1$ ) structure.

<sup>b</sup>From Ref. [9].

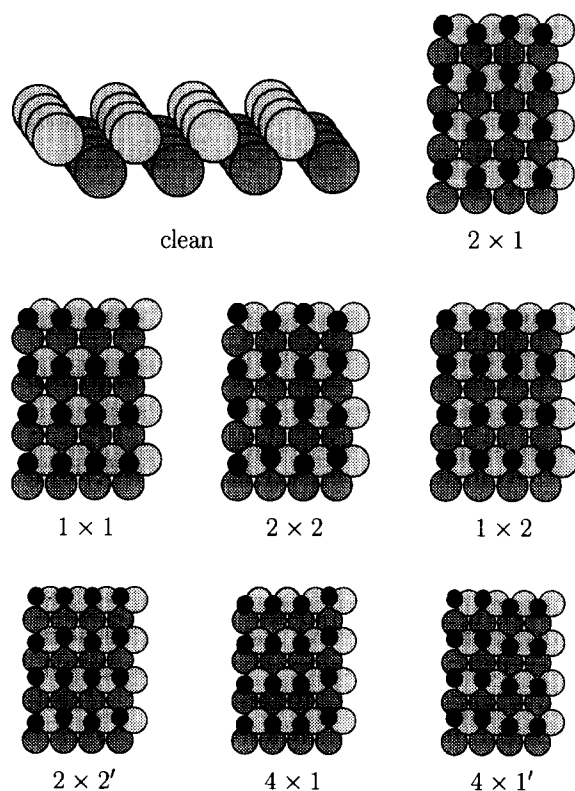


Fig. 1. The seven different surface structures referred to in the text and the clean Rh(110) surface.

stood by a simple qualitative model of the surface energetics which also accounts for the observed ordering of the structures.

In order to disentangle the relative importance

of the adsorbate–substrate and adsorbate–adsorbate interactions, we have modeled the former by a ( $2 \times 2$ ) super-cell in which a single CO molecule is constrained to sit at the same short-bridge site which would be preferred at full coverage. We observe that the dependence of the adsorption energy on  $\alpha$  is very weak up to  $\alpha \approx 10^\circ$ , and that it becomes very steep above this angle. When the coverage increases, the dipole–dipole interaction becomes important and accounts qualitatively for the energy ordering of the structures displayed in Fig. 1. In the ( $2 \times 1$ ) structure, nearest-neighbor molecules are tilted by opposite angles around the axis joining them [the ( $1\bar{1}0$ ) direction], while next-nearest-neighbor molecules are tilted by a same angle about the (001) axis which joins them. The dipole–dipole interaction favors both these arrangements of angles. The ( $2 \times 2$ ) geometry is similar to the previous one as regards the nearest-neighbor interactions, whereas it is unfavored regarding next-nearest-neighbor interactions. The next higher energies are those of the ( $4 \times 1$ ) and ( $4 \times 1'$ ) structures which are almost degenerate because they have the same number of unlike tilt angles along the ( $1\bar{1}0$ ) row. The next structure is the ( $2 \times 2'$ ) one which is characterized by alternating arrangements of energetically favored and disfavored rows and columns of CO molecules. Finally, in the ( $1 \times 1$ ) and ( $1 \times 2$ ) structures the nearest-neighbor molecules are tilted by a same angle and the corresponding dipolar interaction is therefore independent of  $\alpha$ ; it is only the weaker

next-nearest-neighbor interaction which depends on  $\alpha$ . It depends on  $\alpha$  more so for the  $(1 \times 2)$  structure for which the sign of the dipole–dipole interaction energy is the same as that of the adsorbate–substrate interaction, while the two interactions tend to cancel for the other structure. In both cases, this behavior results in a very weak dependence of the energy upon  $\alpha$ , and in an energy degeneracy of the two structures, within our error bars. We have also calculated the adsorption energy of the CO molecules defined as  $E_{\text{slab}}^{\text{Rh-CO}} - E_{\text{slab}}^{\text{Rh}} - E_{\text{slab}}^{\text{CO}}$ , where  $E_{\text{slab}}^{\text{Rh-CO}}$  is the total energy of the CO covered surface,  $E_{\text{slab}}^{\text{Rh}}$  is the total energy of the clean Rh(110) surface, and  $E_{\text{slab}}^{\text{Rh-CO}}$  is the total energy of the CO, all the calculations being done using the same slab geometry and the same set of  $\mathbf{k}$ -points. The calculated adsorption energy is of 2.8 eV per molecule, which has to be compared to the experimental value 1.1 eV per molecule [4]. This large discrepancy is a common feature of the LDA which is well known to overestimate absolute binding energies, whereas equilibrium geometries and energy differences among them are usually predicted with a much higher accuracy (of the order of a few percents).

From Table 1 we see that the energy necessary to tilt the angle of a molecule is of the order of 10–30 meV, whereas the energy difference between different adsorption sites is typically ten times as large. This fact indicates that – for temperatures up to a few hundred K – the relevant configurations which determine thermal equilibrium are all characterized by the molecules staying at their favorite adsorption sites (short-bridge), while differing by their tilt-angle distributions only. Because of this we characterize each configuration by a set of tilt-angles,  $\{\theta_i, \phi_i\}$ , where  $\theta_i$  is the azimuthal angle of the  $i$ th molecule with respect to the (110) direction, and  $\phi_i$  is its polar angle with respect to  $(\bar{1}\bar{1}0)$ . We find that the energy differences among configurations can be accurately modeled by dipolar molecule–molecule interactions up to third-nearest-neighbors and an interaction of each molecule with the substrate of the form

$$B(\theta, \phi) = \cos^2 \phi (a_2 \theta^2 + a_4 \theta^4) + \sin^2 \phi (b_2 \theta^2 + b_4 \theta^4)$$

(dipole model) [22]. We find that  $b$  is about ten times as large as the  $a$ , so that it is a good

approximation to assume that all the molecules are frozen in the positions corresponding to  $\phi = \pm \pi/2$ .

These two values of the  $\phi$  angle can be conveniently labeled by an Ising variable,  $\sigma = \text{sign}(\phi)$ . Much in the same spirit of the *cluster expansion* of the energy landscape of an alloy [23], the energy of each tilt-angle configuration can be expressed in terms of polynomials in the  $\sigma$ s [24]. Because of the symmetry, odd-power polynomials are absent from the cluster expansion. Restricting ourselves to second-order polynomials (spin-pair interactions) and neglecting all the couplings beyond the next-nearest-neighbors, the cluster expansion of the surface energy would read:

$$E[\{\sigma\}] = \frac{1}{2} \sum_{i,j} \sigma_{i,j} \left( J_x \sum_{\delta=\pm 1} \sigma_{i+\delta,j} + J_y \sum_{\delta=\pm 1} \sigma_{i,j+\delta} + J_2 \sum_{\delta,\delta'=\pm 1} \sigma_{i+\delta,j+\delta'} \right), \quad (1)$$

It is straightforward to see that:

$$\begin{aligned} E_{2 \times 1} &= J_y - J_x - 2J_2, & E_{1 \times 1} &= J_x + J_y + 2J_2, \\ E_{1 \times 2} &= J_x - J_y - 2J_2, & E_{2 \times 2} &= 2J_2 - J_y - J_x, \\ E_{4 \times 1} &= E_{4 \times 1'} = J_y, & E_{2 \times 2'} &= 0. \end{aligned} \quad (2)$$

where the subscripts refer to the structures of Fig. 1.

$E_{2 \times 1}$  is the ground-state energy which we take as the reference energy. The  $(4 \times 1)$  and  $(4 \times 1')$  structures are degenerate within the present model, and their energy difference provides therefore an estimate of longer-range or many-spin interactions which have been neglected. From Eq. (2), one can extract four independent energy differences, which are linear functions of the three parameters  $J_x$ ,  $J_y$ , and  $J_2$ . By disregarding one of these equations in turn, one obtains four different linear systems for  $J$  that provide different estimates for these parameters, which coincide within  $\approx 1$  meV. The average of the four sets of parameters so obtained is:  $J_x = 13.6$  meV,  $J_y = -3.4$  meV, and  $J_2 = 1.7$  meV. Note the large difference between the absolute values of  $J_x$  and  $J_y$ , which is due to a stronger coupling in the “ziz-zag”  $(\bar{1}\bar{1}0)$  direction, where the distance between neighboring molecules

is smaller by a factor  $\sqrt{2}$  than in the orthogonal direction.

The thermal properties of our system are obtained by standard Metropolis Monte Carlo simulations of the above Ising model (see for example Ref. [25]). To this end, we have used a  $32 \times 32$  square lattice with periodic boundary conditions. The order parameter of the transition between the  $(2 \times 1)$  ordered phase and the disordered phase where the tilt-angles are distributed at random, is the Fourier coefficient of the spin–spin correlation function,  $M(\mathbf{q}) = (1/N) \sum_r e^{i\mathbf{q} \cdot \mathbf{r}} \langle \sigma_r \sigma_0 \rangle$  at wavevector  $\mathbf{q} = (\pi, 0)$ ,  $M \equiv M(\pi, 0)$ . The order–disorder transition temperature,  $T_c^{\text{Is}}$ , is estimated looking at the maximum of the specific heat  $C$ . We have not attempted any finite-size scaling, but we have verified that the location of the transition temperature is rather insensitive to the choice of the size of the system, by making a few simulations for a  $64 \times 64$  system. In Fig. 2 we show the behavior of the specific heat,  $C$ , and the order parameter,  $M$ , as functions of temperature. Also shown in Fig. 2 is a comparison between the specific heats as calculated from the simulations of the Ising model and from an independent simulation performed for the dipole model described above. The Ising critical

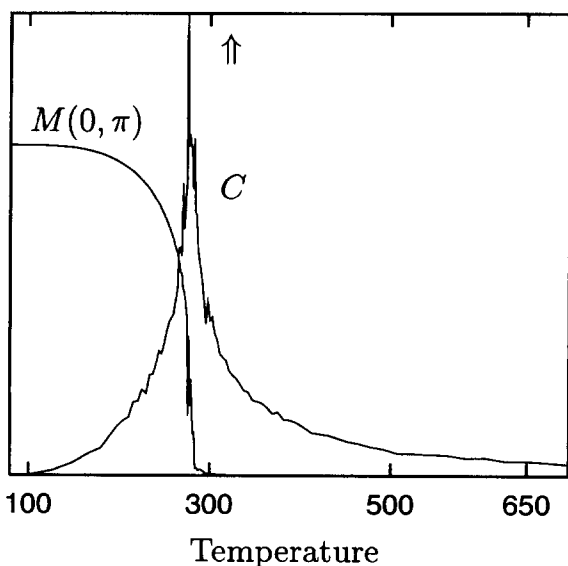


Fig. 2. Fourier transform of the correlation function for the two-dimensional spin model and specific heat for the spin and dipole models (see text).

temperature is  $T_c^{\text{Is}} = 280$  K, while for the dipole model it is  $T_c^{\text{dip}} = 340$  K. The statistical error on these critical temperatures is of a few degrees only. Based on these figures and on a rough estimate of the dependence of the transition temperatures upon the value of the parameters of the two models, we conclude that an order–disorder  $(2 \times 1) \rightarrow (1 \times 1)$  transition occurs at a critical temperature of  $T_c \approx 300$  K with an error bar  $< 100$  K. The simulations were done starting at a high temperature ( $T > 650$  K) and cooling down the system by small temperature steps ( $\approx 2$  K). When the temperature reached  $\approx 50$  K, well below the formation of the ordered structure, we heated up the system using the same temperature steps. For every size of the simulation lattice we observed no hysteresis. This fact is an indication of the second-order character of the transition.

We have studied from first principles and Monte Carlo simulations the Rh(110) surface covered by one monolayer of CO molecules. In agreement with experimental data we found that the  $(2 \times 1)$ p2mg structure is the most stable, with the molecules arranged in the short-bridge site in a “zig-zag” fashion. The experimental claim made in Ref. [6] of a possible order–disorder transition is supported by our results which indicate a critical temperature for this transition of  $T_c \approx 300$  K, in good agreement with the experimental findings.

### Acknowledgements

The ab initio calculations were performed on the SISSA IBM-SP2 (16 processors) in Trieste and on the CINECA-INFM Cray-T3D (128 processors) in Bologna using the parallel version of the PWSCF code.

### References

- [1] G. Comelli, V.R. Dhanak, M. Kiskinova, N. Pangher, G. Paolucci, K.C. Prince, R. Rosei, Surf. Sci. 260 (1992) 7; Surf. Sci. 269/270 (1992) 360.
- [2] V.R. Dhanak, G. Comelli, G. Cautero, G. Paolucci, M. Kiskinova, K.C. Prince, R. Rosei, Chem. Phys. Lett. 188 (1992) 237.

- [3] D. Alfè, P. Rudolf, M. Kiskinova, R. Rosei, Chem. Phys. Lett. 211 (1993) 220.
- [4] M. Bowker, Q. Guo, R. Joyner, Surf. Sci. 253 (1991) 33.
- [5] V. Schmatloch, N. Kruse, Surf. Sci. 269/270 (1992) 488.
- [6] A. Baraldi, V.R. Dhanak, G. Comelli, K.C. Prince, R. Rosei, Surf. Sci. 293 (1993) 246.
- [7] V.R. Dhanak, A. Baraldi, G. Comelli, G. Paolucci, M. Kiskinova, R. Rosei, Surf. Sci. 295 (1993) 287.
- [8] L. Casalis, A. Baraldi, G. Comelli, V.R. Dhanak, M. Kiskinova, R. Rosei, Surf. Sci. 306 (1994) 193.
- [9] J.D. Batteas, A. Barbieri, E.K. Starkey, M.A. Van Hove, G.A. Somorjai, Surf. Sci. 313 (1994) 341.
- [10] J.J. Weimer, J. Loboda-Cackovic, J.H. Block, Surf. Sci. 316 (1994) 123.
- [11] K.C. Prince, A. Santoni, A. Morgante, G. Comelli, Surf. Sci. 317 (1994) 397.
- [12] R. Gómez, A. Rodes, J.M. Péres, J.M. Feliu, A. Aldaz, Surf. Sci. 327 (1995) 202.
- [13] P. Hohenberg, W. Kohn, Phys. Rev. 136 (1964) B864.
- [14] W. Kohn, L. Sham, Phys. Rev. 140 (1965) A1133.
- [15] D. Ceperley, B. Alder, Phys. Rev. Lett. 45 (1980) 566.
- [16] D. Vanderbilt, Phys. Rev. B 41 (1990) 7892.
- [17] K. Stokbro, Phys. Rev. B 53 (1996) 6869.
- [18] K. Stokbro, S. Baroni, Surf. Sci., to be published.
- [19] M. Methfessel, A. Paxton, Phys. Rev. B 40 (1989) 3616.
- [20] H.J. Monkhorst, J.D. Pack, Phys. Rev. B 13 (1976) 5188.
- [21] W. Nichtl, N. Bickel, L. Hammer, K. Heinz, K. Müller, Surf. Sci. 188 (1987) L729.
- [22] We have performed our fit by allowing the strength of the dipole–dipole interaction to depend on the order of neighbor. We have used a data set of thirteen structures and obtained a mean square error between fitted and calculated energies of 1.5 meV per molecule, with a maximum error of 3 meV. The error in the equilibrium value of the  $\theta$  angle is of the order of a few degrees.
- [23] J.W.D. Connolly, A.R. Williams, Phys. Rev. B 27 (1983) 5169.
- [24] We associate to each given distribution of Ising variables,  $\{\sigma_i\}$ , an energy defined as the minimum with respect to the  $\theta$ s of the energy calculated at fixed  $\phi$ s:  $E[\{\sigma_i\}] \equiv \min_{\theta} E[\langle \theta, \sigma(\pi/2) \rangle]$ .
- [25] D. Chandler, Introduction to Modern Statistical Mechanics, Oxford University Press, Oxford, 1987.